catalysts

MDPI

Supplementary material

An escape from noble metals for generating urethanes via reductive carbonylation of nitroarenes over $FeSe_2/\gamma\text{-}Al_2O_3$

Anh Vy Tran [1], Thuy Tram Huynh Nguyen [1], Thanh Tung Nguyen [1], Jayeon Baek [2], and Yong Jin Kim[2,*]

[1] Department of Green Process and System Engineering, Korea University of Science and Technology (UST), 89 Yangdaegiro-gil, Ipjang-myeon, Cheonan 31056, Republic of Korea

[2] Green Chemistry & Material Group, Korea Institute of Industrial Technology, 89 Yangdaegiro-gil, Cheonan-si 31056, Republic of Korea

* Correspondence: yjkim@kitech.re.kr (Y. J. Kim); Tel: (+82-41) 589-8469; fax: (+82-41) 589-8580

Supplementary Materials: The following are available online at www.mdpi.com/xxx/s1, Figure S1: title, Table S1: title, Video S1: title.

Contents:

15. ^{1}H-NMR spectra of MPC product obtained from the reductive carbonylation reaction (Fig. S13)
16. ^{13}C-NMR spectra of MPC product obtained from the reductive carbonylation reaction (Fig. S14)
17. GC-MS of Methyl (4-methoxyphenyl) carbamate (Fig. S15)
18. GC-MS of Methyl (4-methylphenyl) carbamate (Fig. S16)
19. GC-MS of Methyl (4-bromophenyl) carbamate (Fig. S17)
20. GC-MS of Methyl (4-acetylphenyl) carbamate (Fig. S18)
21. GC-MS of Dimethyltoluene-2,4-dicarbamate (Fig. S19)
22. GC-MS of Dimethyl 1,4-phenylenebiscarbamate (Fig. S20)
23. SEM images of fresh $FeSe_2$/ γ-Al_2O_3 catalyst, and spent $FeSe_2$/ γ-Al_2O_3 (Fig. S21)
24. X-ray diffraction spectra of (a) fresh catalyst $FeSe_2$, and (b) recovered $FeSe_2$ (Fig. S22)
25. X-ray photoelectron spectroscopy (XPS) of the fresh and spent $FeSe_2$/ γ-Al_2O_3 (Fig. S23)

Table S. 1 Different types of $FeSe_2$/support for the formation of MPC[a]

Entry	Catalyst	NB Conversion (%)	MPC Yield (%)	Selectivity (%)
1	$FeSe_2$/ γ-Al_2O_3	>99	98.9	98.9
2	$FeSe_2$/ basic Al_2O_3	>99	91.6	91.6
3	$FeSe_2$/ α-Al_2O_3	98.1	87.8	89.5
4	$FeSe_2$/$AlPO_4$	87.0	85.7	98.5
5	$FeSe_2$/Zeolite beta	>99	79.9	79.9
6	$FeSe_2$/Activated C	>99	75.9	75.9
7	$FeSe_2$/SiO_2	78.4	71.5	91.3
8	$FeSe_2$/CeO_2	78.2	65.5	83.7
9	$FeSe_2$/neutral Al_2O_3	71.6	64.6	90.3
10	$FeSe_2$/FA-PO_4	59.4	58.1	97.9
11	$FeSe_2$/acidic Al_2O_3	60.8	49.7	81.7
12	$FeSe_2$/Montmorillonite	50.8	43.2	85.0

[a]NB (2.46 g, 20 mmol), 4~5 wt% $FeSe_2$/support (1 g, [$FeSe_2$]: 0.2338 mmol), molar ratio of NB/$FeSe_2$ = 85, MeOH (30 mL), T = 160 °C, P (CO) = 8.3 MPa, *t* = 4 h.

Table S. 2 TON value of the reductive carbonylation reaction using $FeSe_2/\gamma\text{-}Al_2O_3$ as catalyst

Entry	Substrate	gNB / g$FeSe_2$	Molar ratio NB/$FeSe_2$	TON (wt)	TON (mmol)
1[a]	NB	560	1000	221	384
2[b]	NB:ANL (1:1)	560	1000	369	640

[a]Conditions: NB (7.2 g, 58.5 mmol), 5wt% $FeSe_2/\gamma\text{-}Al_2O_3$ (0.25 g, [$FeSe_2$] = 0.0125 g, 0.0585 mmol), molar ratio of NB/$FeSe_2$= 1000, MeOH = 30 mL, P = 8.3MPa of CO, T = 160 °C, *t* = 72 h.

[b] NB (7.2 g, 58.5 mmol), AN (5.45 g, 58.5 mmol), 5wt% $FeSe_2/\gamma\text{-}Al_2O_3$ (0.25 g, [$FeSe_2$] = 0.0125 g, 0.0585 mmol), MeOH = 30 mL, P = 8.3MPa of CO, T = 160 °C, *t* = 72 h.

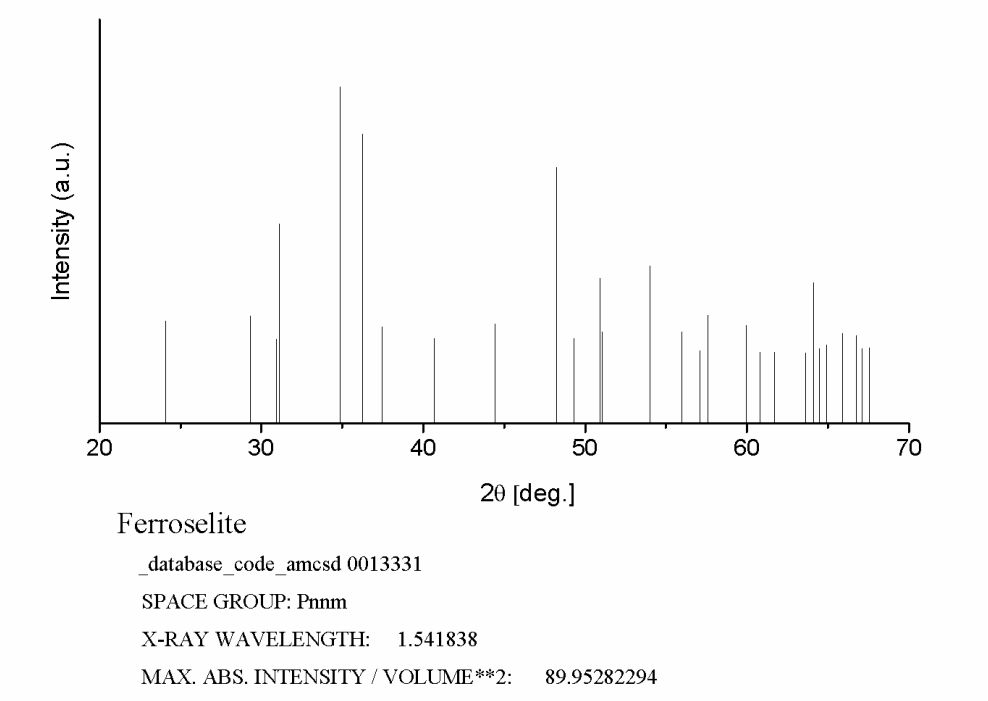

Figure S. 1 X-ray diffraction spectra (XRD) of standard Ferroselite $FeSe_2$

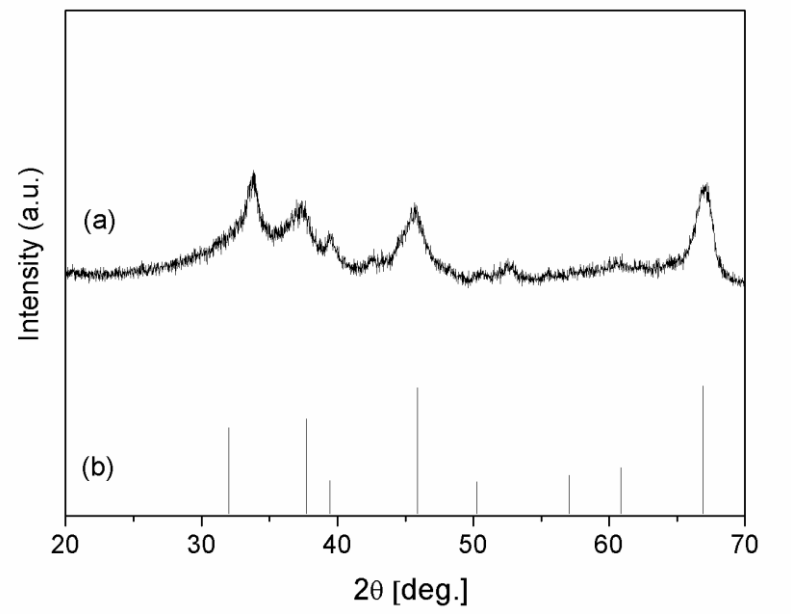

Figure S. 2 (a) X-ray diffraction spectra (XRD) of $FeSe_2/\gamma$ Al_2O_3, (b) XRD standard spectra of $Al_{2.144}O_{3.2}$ (γ - Aluminium oxide) PDF-number 79-1558-Cubic Fd-3m (227)

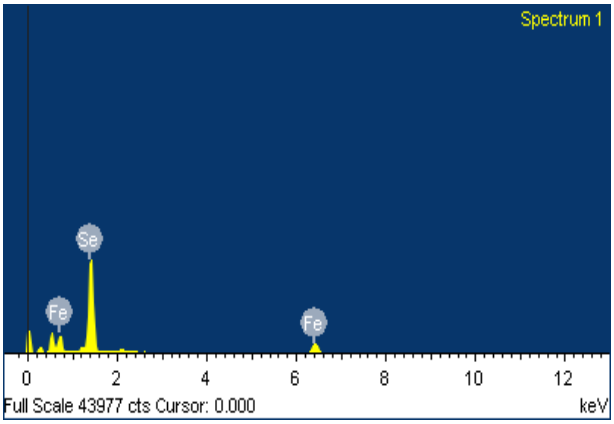

Element	Weight%	Atomic%
Fe K	24.90	31.91
Se L	75.10	68.09
Totals	100.00	

Figure S. 3 EDX/EDS spectra of $FeSe_2$ and the atomic ratio calculation of Fe/Se.

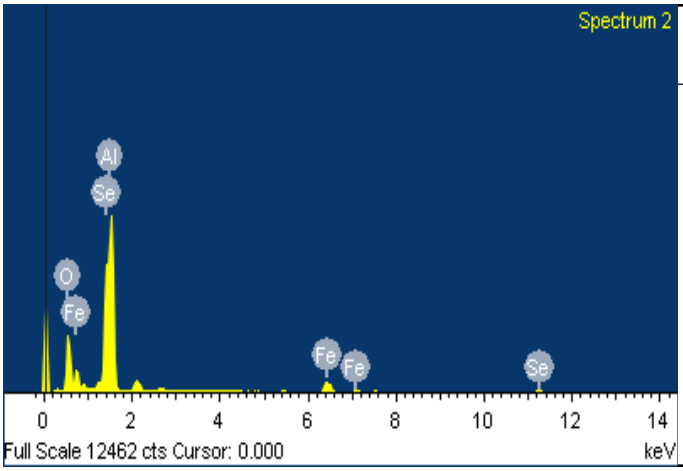

Element	Weight%	Atomic%
Fe K	1.23	0.46
Se L	3.15	0.83
Al K	49.51	38.28
O K	46.11	60.32
Totals	100.00	

Figure S. 4 EDX/EDS spectra of $FeSe_2/\gamma$-Al_2O_3 and the atomic ratio calculation.

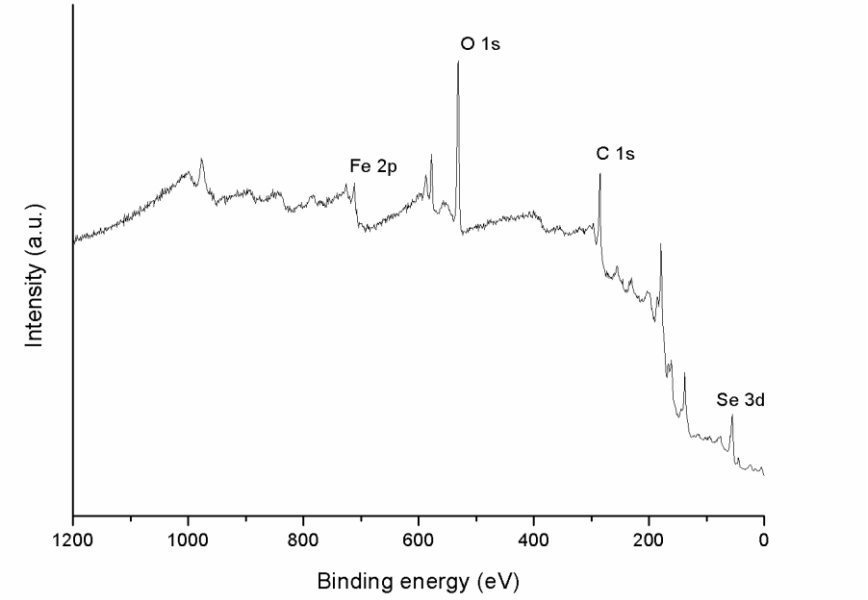

Figure S. 5 X-ray photoelectron spectroscopy (XPS) survey spectra of $FeSe_2$

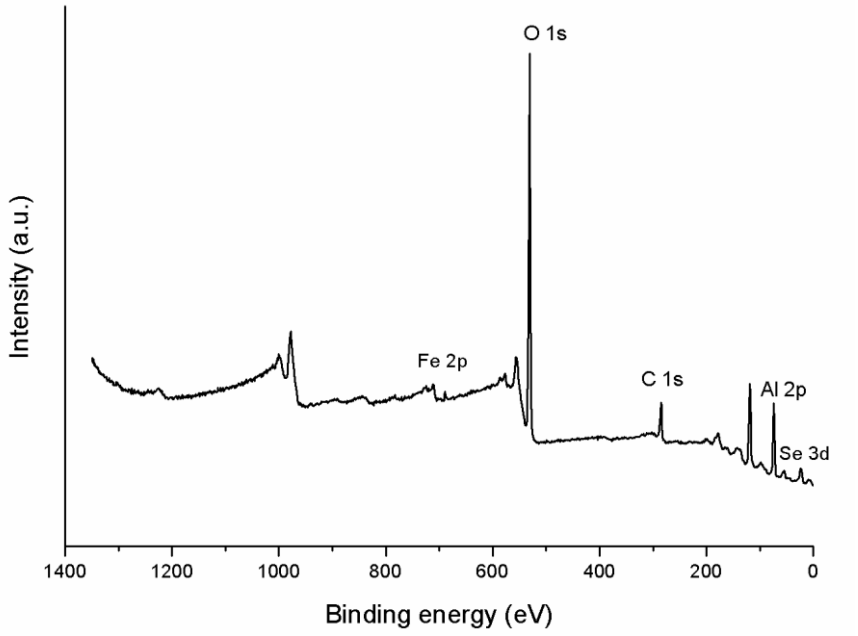

Figure S. 6 X-ray photoelectron spectroscopy (XPS) survey spectra of $FeSe_2/\gamma\ Al_2O_3$

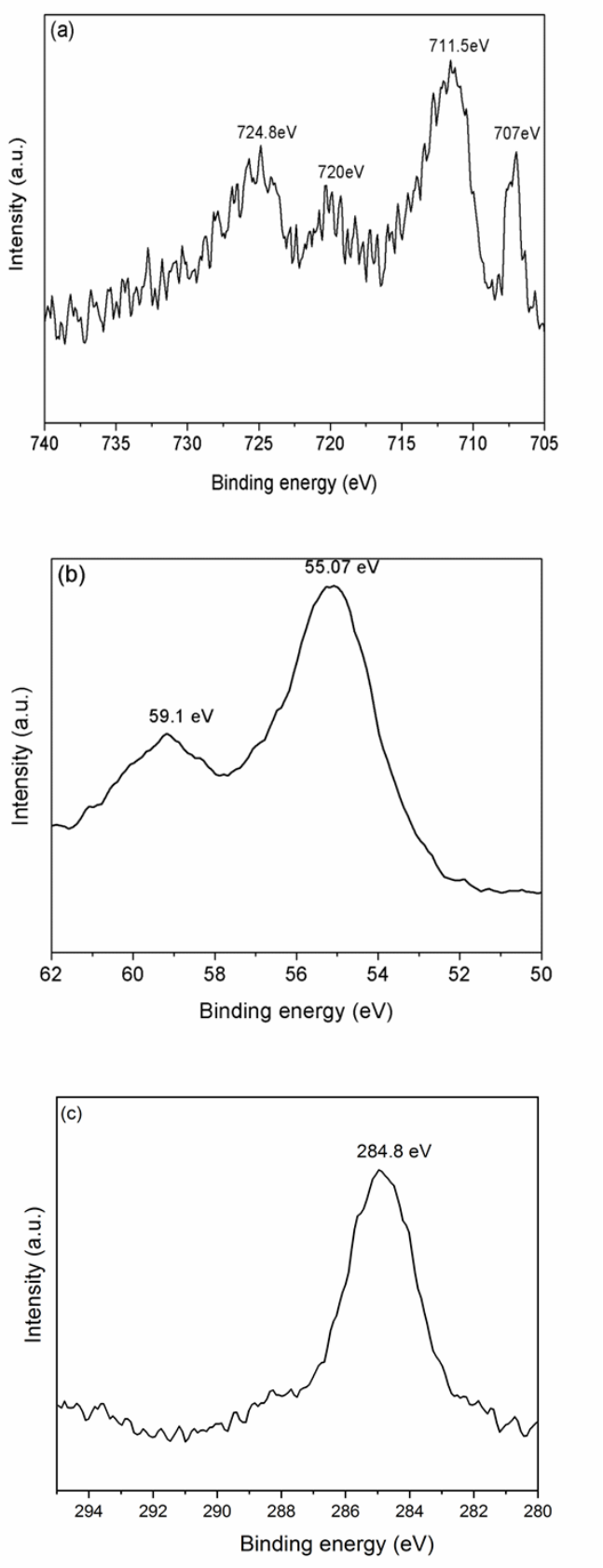

Figure S. 7 . X-ray photoelectron spectroscopy (XPS) spectra of $FeSe_2$ in the region of (a) Fe3p, (b) Se3d, and (c) C1s.

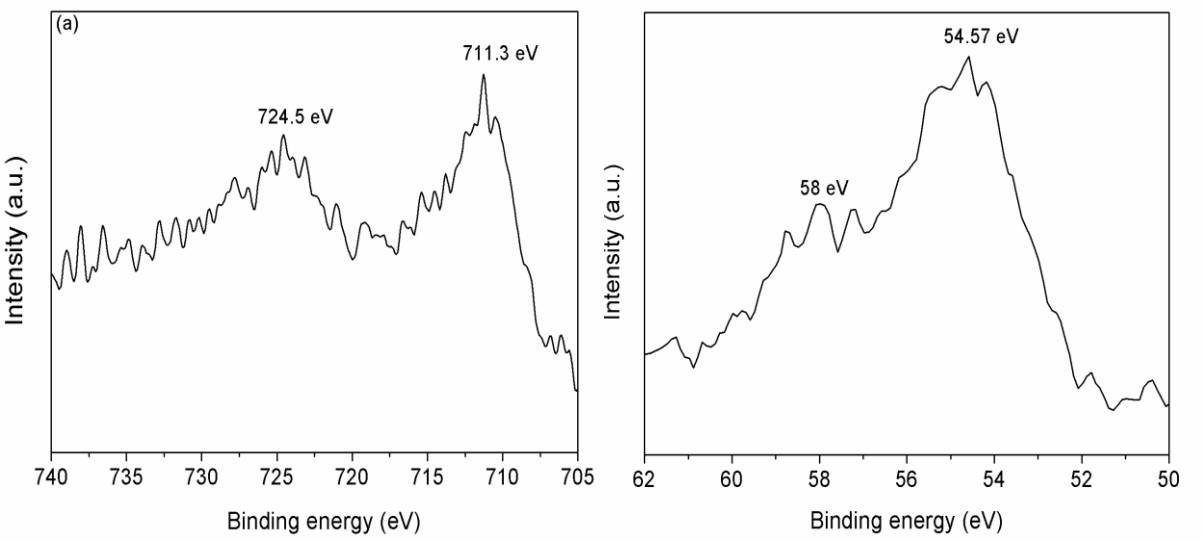

Figure S. 8 X-ray photoelectron spectroscopy (XPS) of $FeSe_2$/ γ-Al_2O_3 in the region of (a) Fe3p and (b) Se3d

XPS analysis was carried out to investigate the oxidation state of Fe and Se in $FeSe_2/\gamma$ -Al_2O_3. XPS survey spectra of $FeSe_2/\gamma$-Al_2O_3, (see Fig.S-6) shows the photoelectron lines of Fe, Se, Al, and O. In Fig S.7a, two peaks of Fe $2p_{1/2}$ and Fe $2p_{3/2}$ at 711.3 and 724.5 eV clearly indicates the existence of Fe^{2+}, which is well in accordance with the literature [1]. Meanwhile, the peak at 54.57 eV and 58 eV in Fig.S7b can be ascribed to Se $3d_{5/2}$ and Se $3d_{3/2}$, indicating the existence of Se_2^{2-} species in the $FeSe_2$ [1-3]. From these data, it is clear that the $FeSe_2$ after loading on support appeared with binding energy values almost the same as those values of the neat $FeSe_2$.

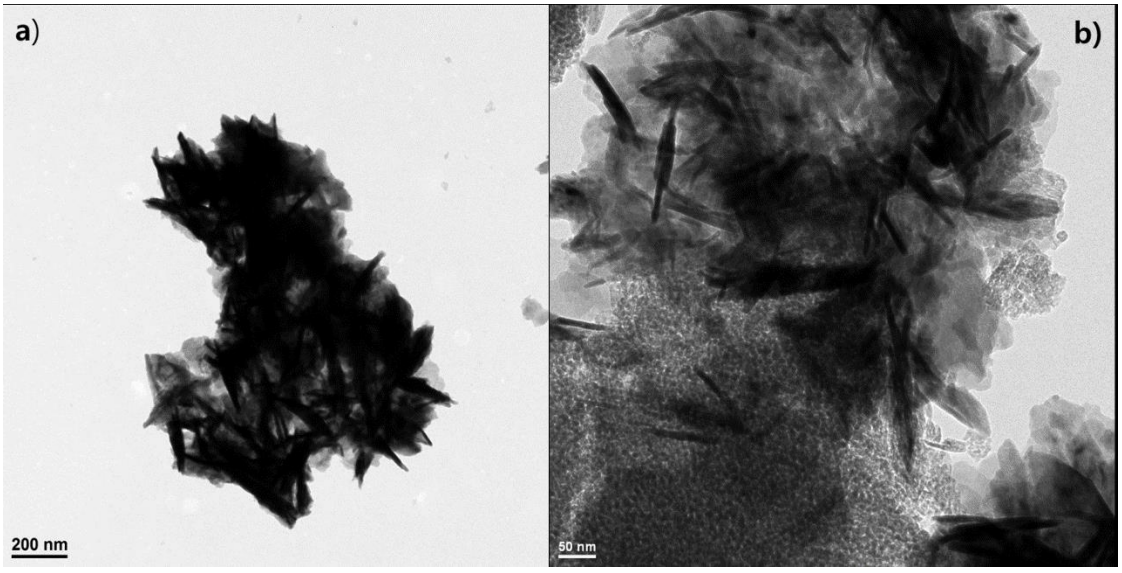

Figure S.9 High resolution TEM images of (a) neat $FeSe_2$ prepared with the presence of pyridine, and (b)

$FeSe_2/\gamma\text{-}Al_2O_3$ prepared with the presence of pyridine.

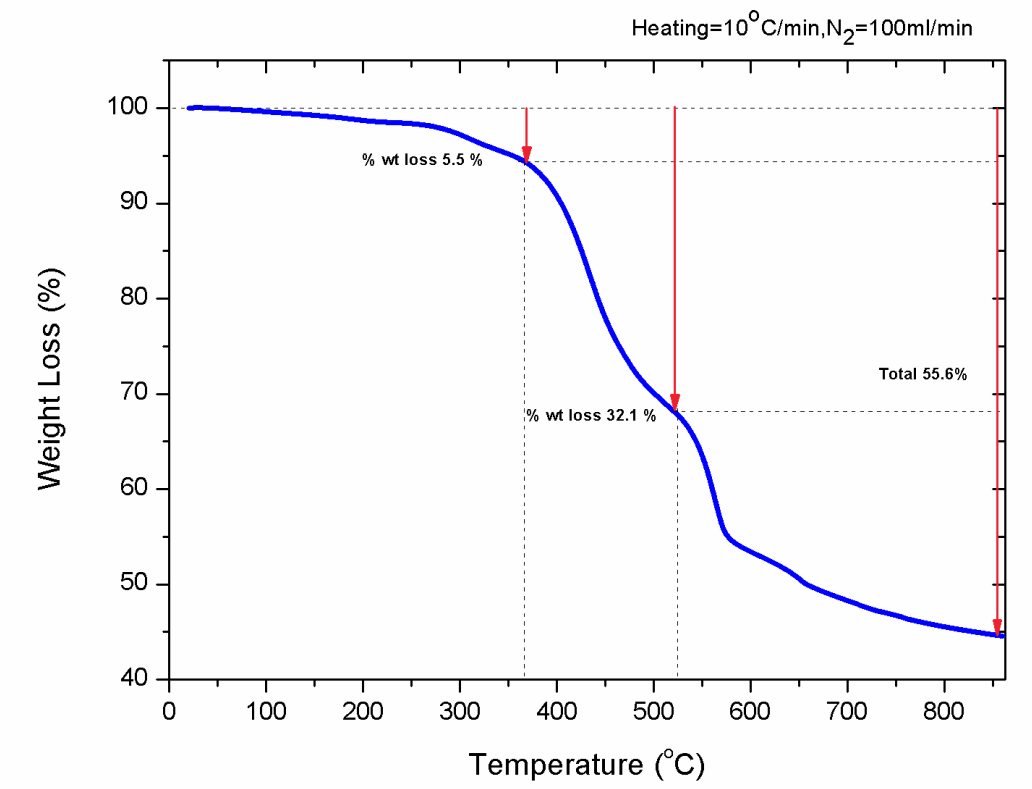

Figure S. 10 Thermogravimetric analysis (TGA) of $FeSe_2$.

Thermal stability of neat $FeSe_2$ as prepared catalyst is confirmed by TGA. The fig S.9 shows that the major mass loss started from 380 to 520 °C is due to the decomposition of $FeSe_2$. It is indicating that $FeSe_2$ have high thermal stability up to 380 °C.

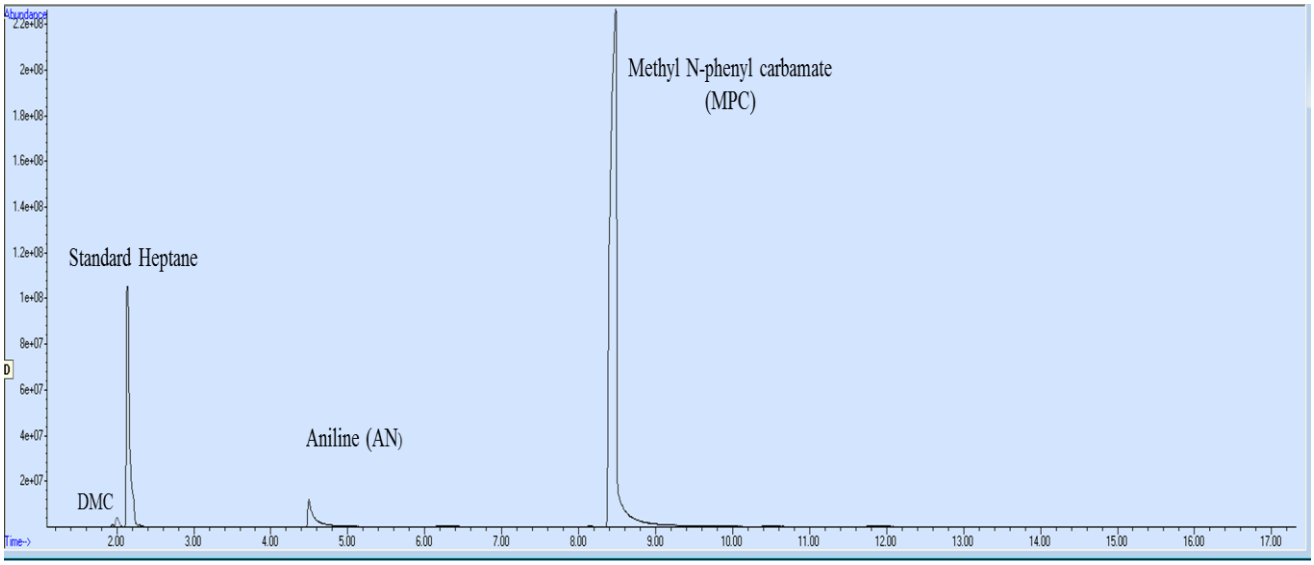

Figure S. 11 GC-MS of the filtrate obtained in the reductive carbonylation reaction using $FeSe_2$ as catalyst with molar ratio NB/$FeSe_2$ = 1,

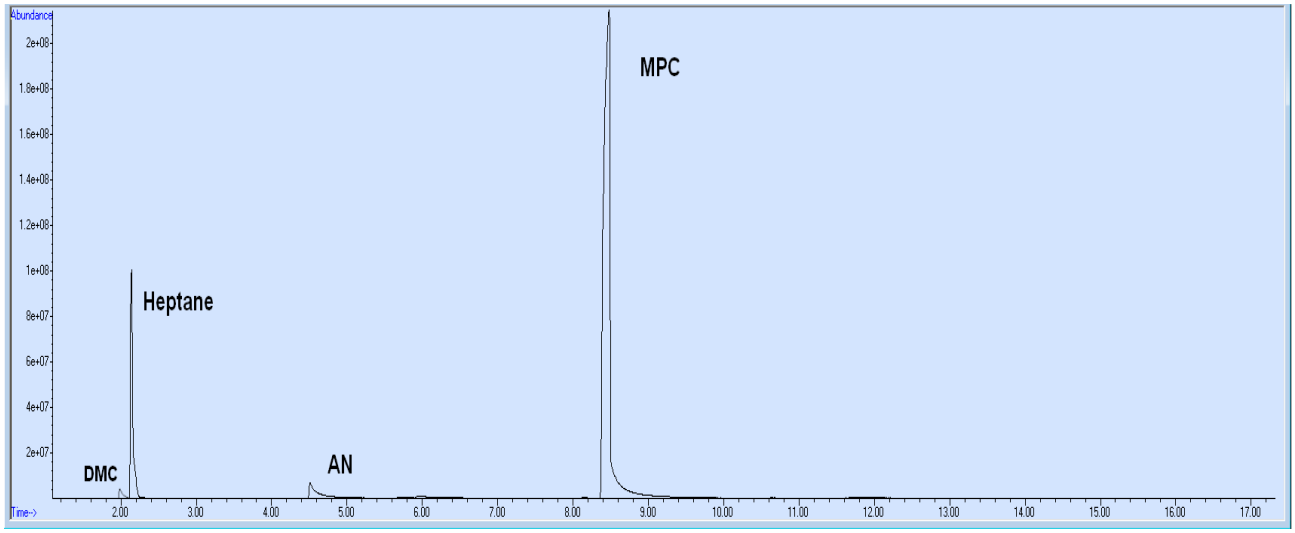

Figure S. 12 GC-MS of the filtrate obtained in the reductive carbonylation reaction using $FeSe_2$ as catalyst with molar ratio NB/$FeSe_2$ = 4

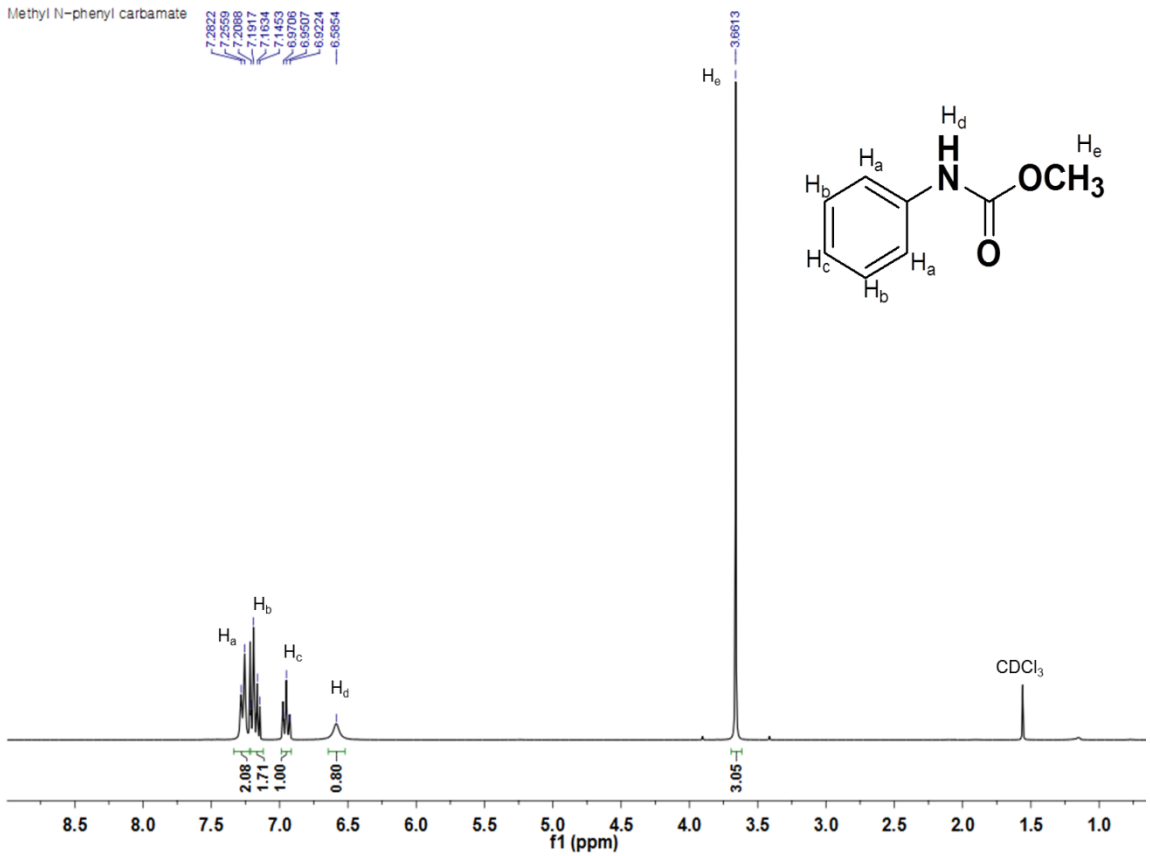

Figure S. 13 ^{1}H-NMR spectra of Methyl N-phenyl carbamate (MPC) product obtained from the reductive carbonylation rxn. ^{1}H NMR (300 MHz, $CDCl_3$, δ 3.66 (s, 3H, OCH_3); 6.59 (s, 1H, NH); 6.95 (t, 1H, ArH); 7.17(m, 2H, ArH); 7.27 (d, 2H, ArH).

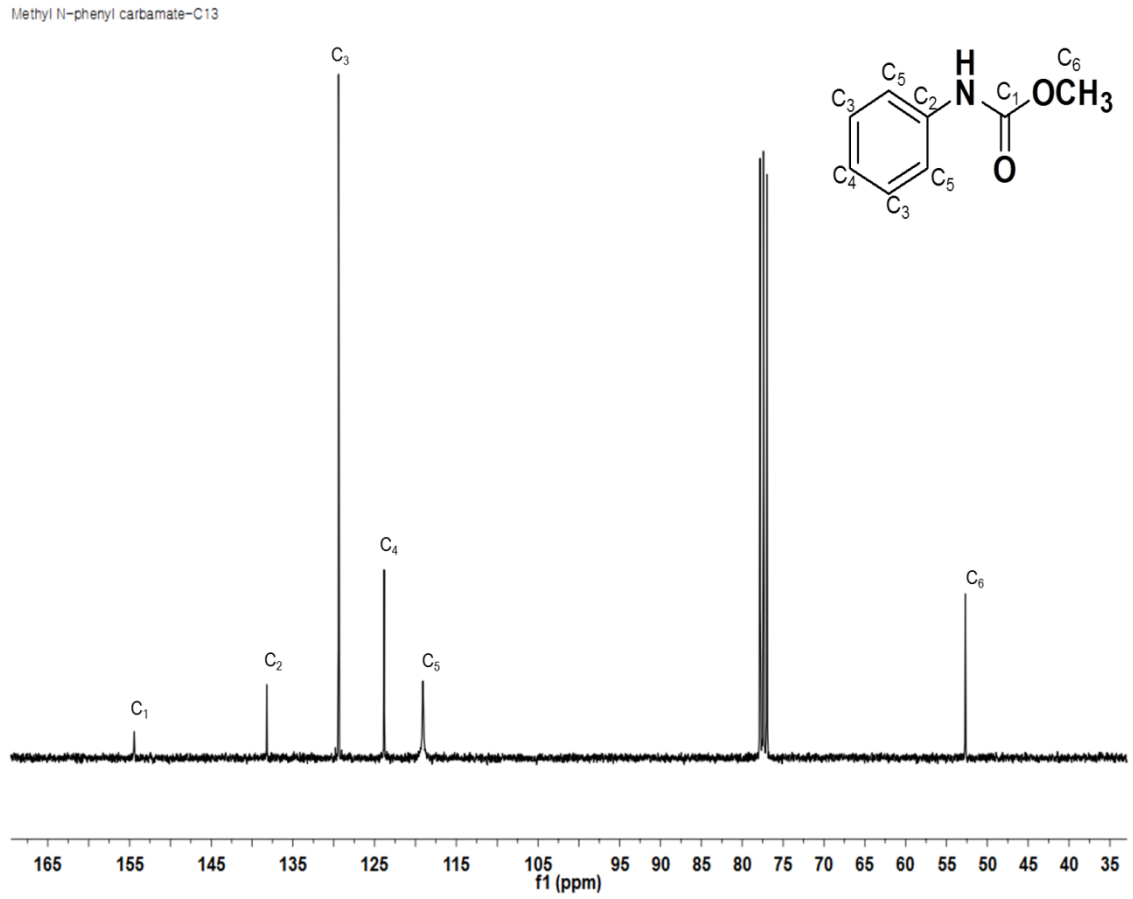

Figure S. 14 ^{13}C-NMR of MPC product obtained from the reductive carbonylation reaction of nitrobenzene. ^{13}C NMR (300 MHz, $CDCl_3$, δ 52.5 (OCH_3); 118.85 (C_6H_5-); 123.6 (C_6H_5-); 129.1 (C_6H_5-); 137.9 (C_6H_5-); 154.19 (C_6H_5-).

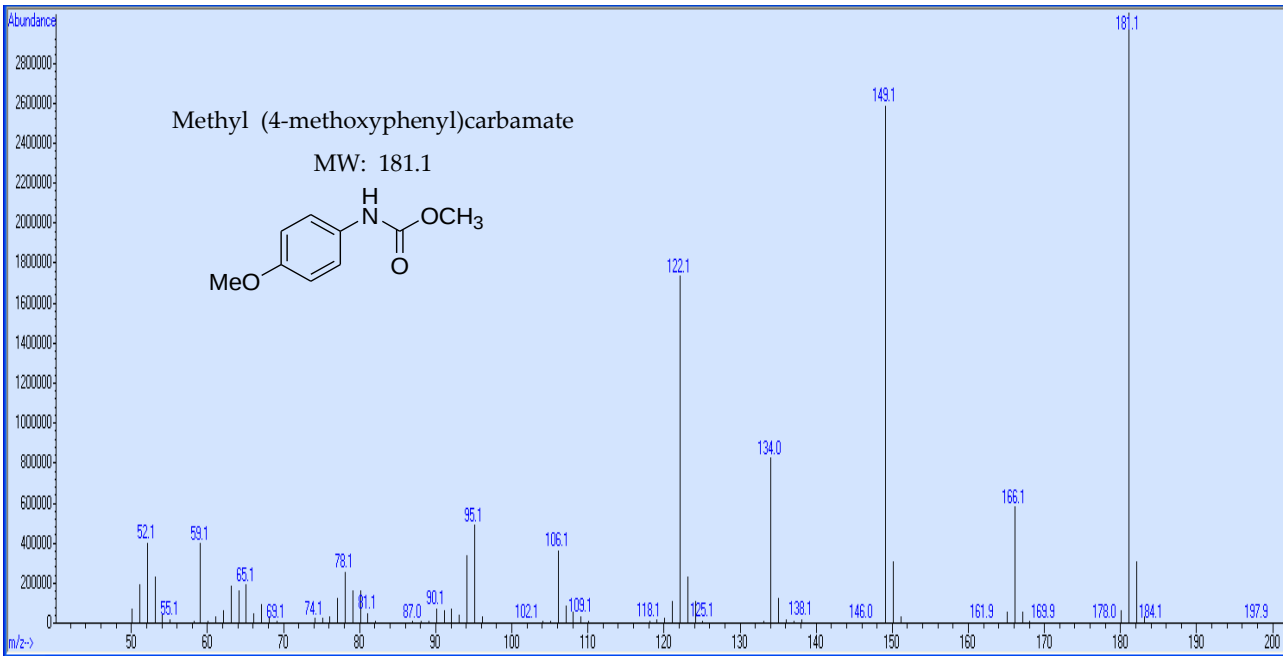

Figure S. 15 GC-MS of Methyl (4-methoxyphenyl) carbamate

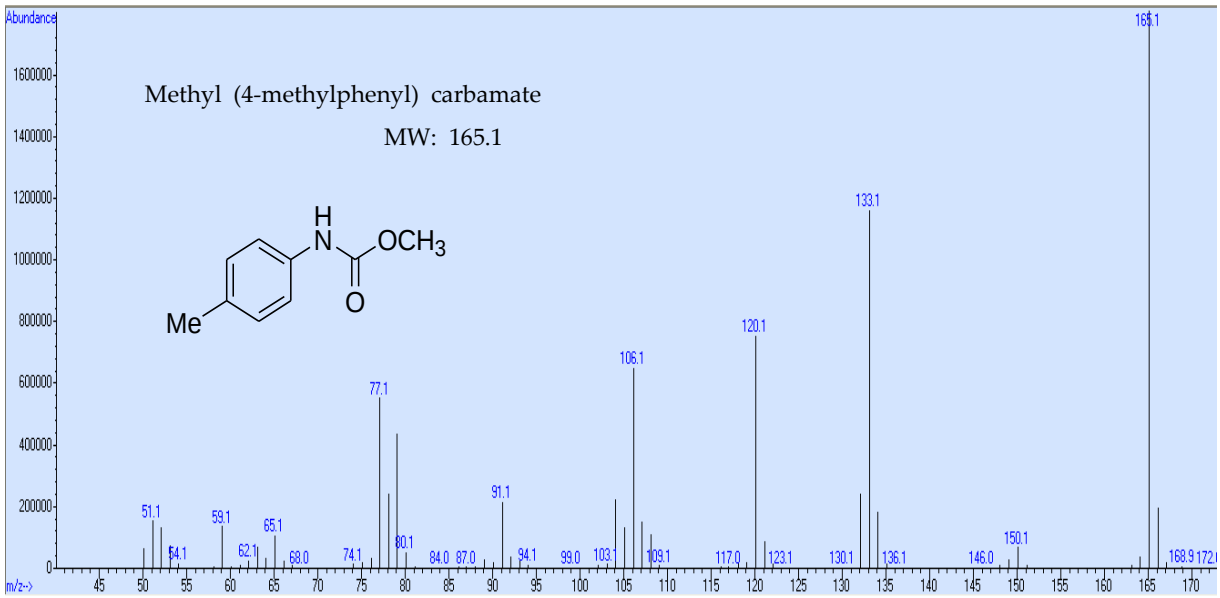

Figure S. 16 GC-MS of Methyl (4-methylphenyl) carbamate

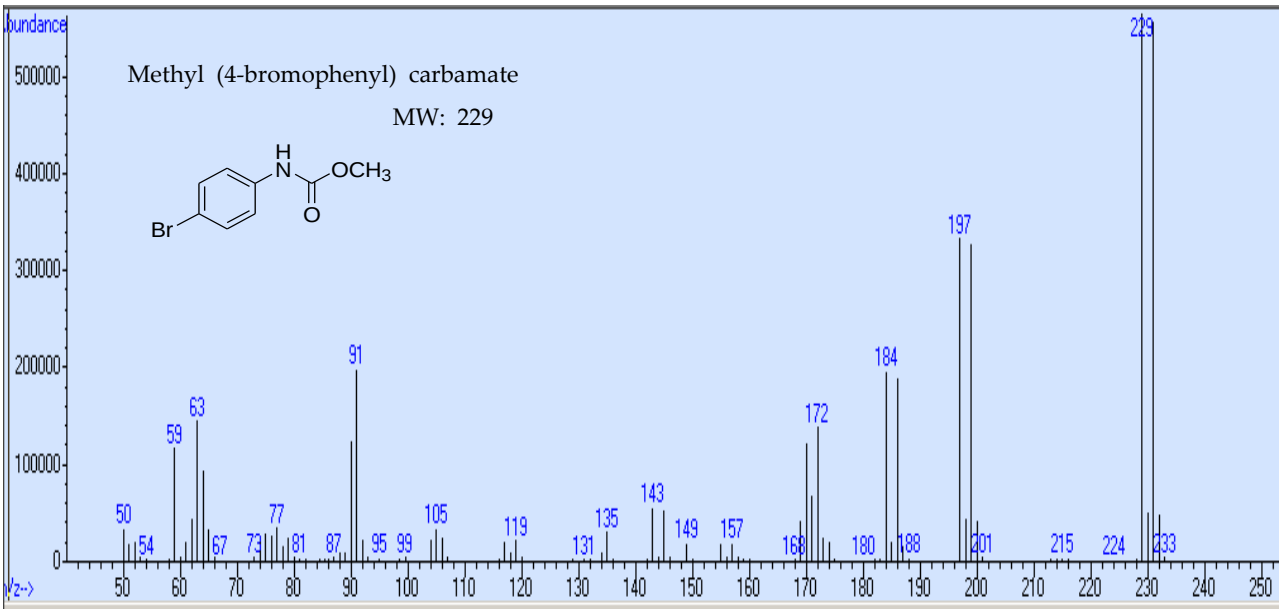

Figure S. 17 GC-MS of Methyl (4-bromophenyl) carbamate

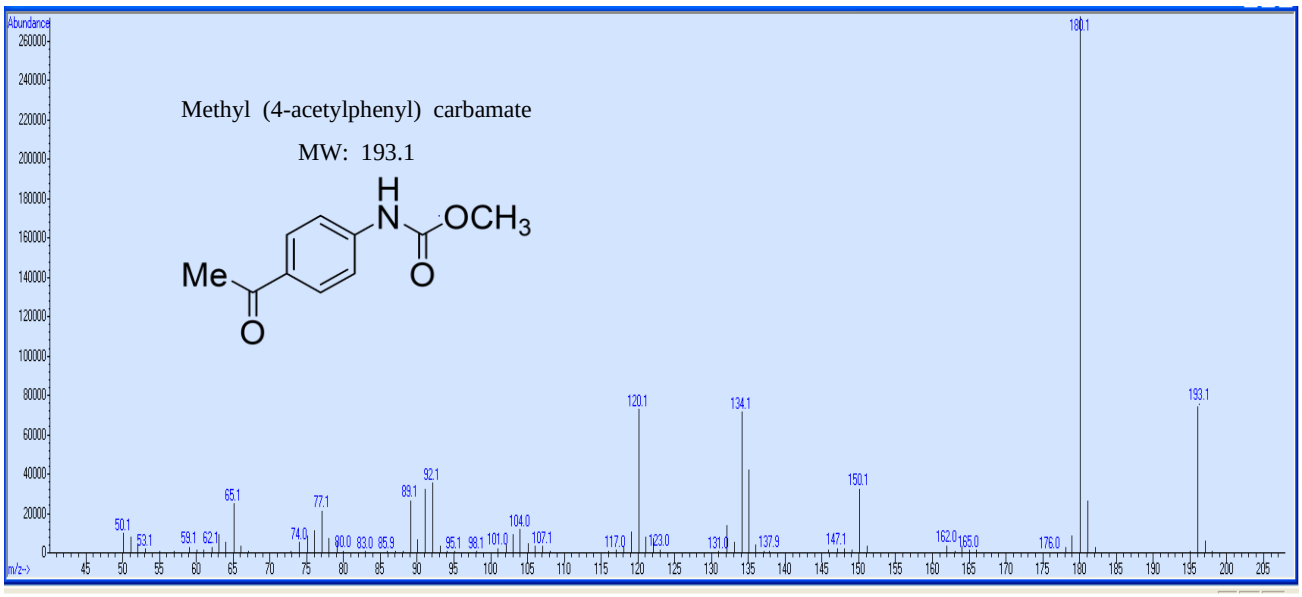

Figure S. 18 GC-MS of Methyl (4-acetylphenyl) carbamate

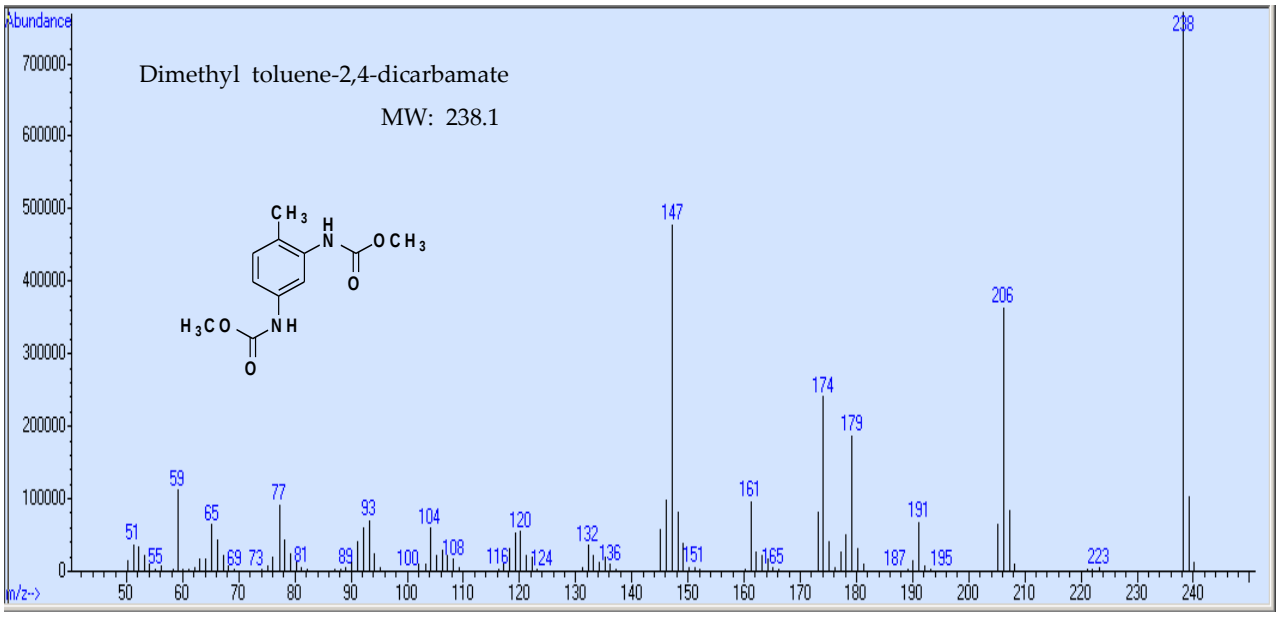

Figure S. 19 GC-MS of Dimethyl toluene-2,4-dicarbamate

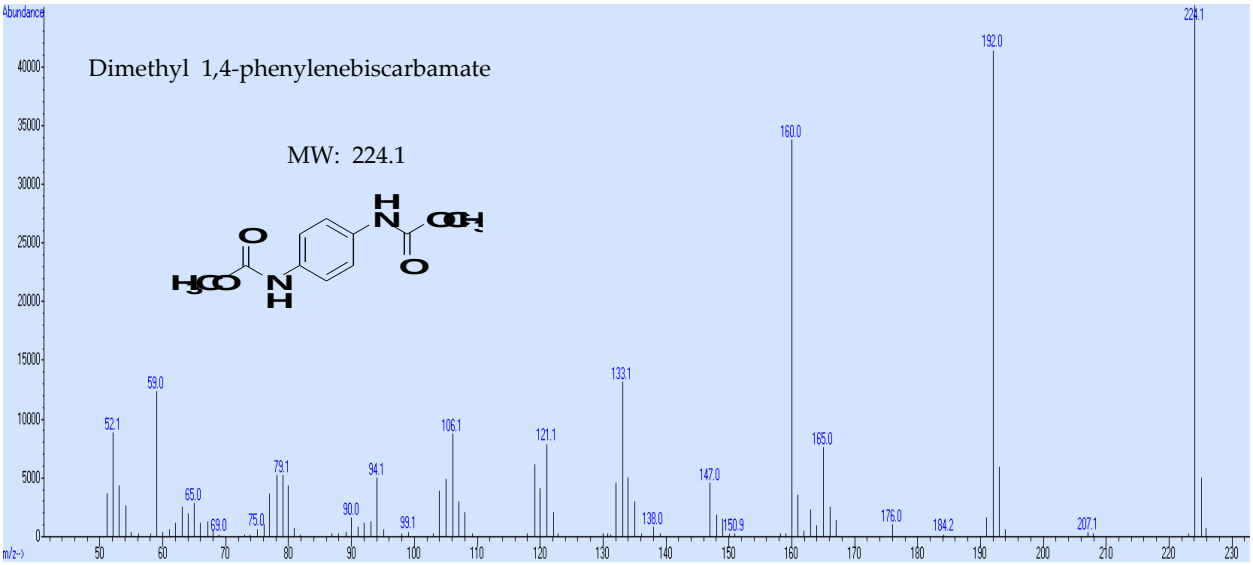

Figure S. 20 GC-MS of dimethyl 1,4-phenylenebiscarbamate

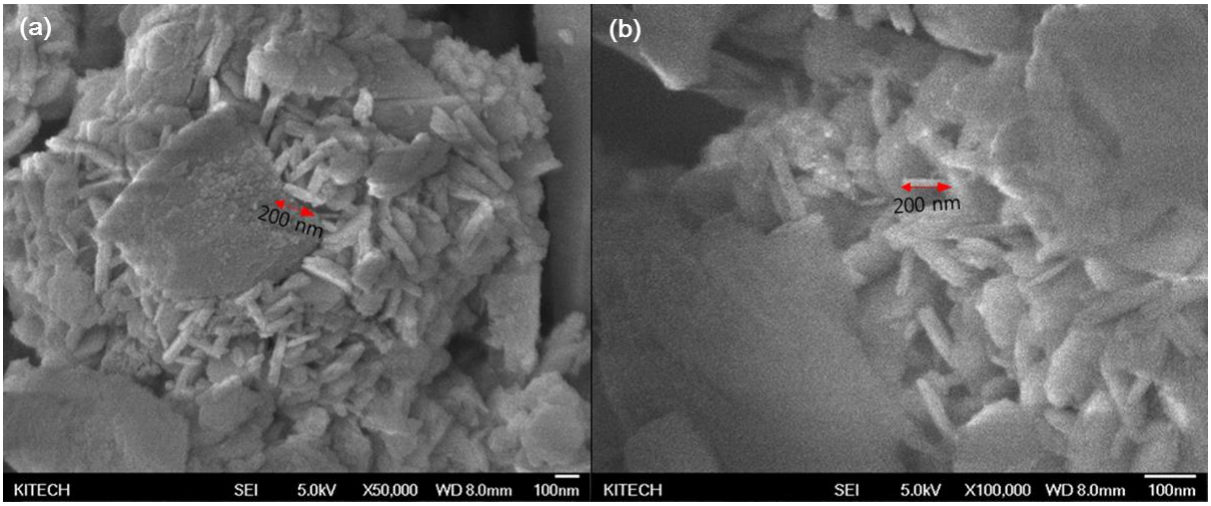

Figure S. 21 Scanning electron microscopy (SEM) figures of (a) fresh $FeSe_2/\gamma\text{-}Al_2O_3$ catalyst, and (b) spent $FeSe_2/\gamma\text{-}Al_2O_3$

As shown in Fig. S20, SEM analysis was conducted to compare the morphology of the fresh and reused catalysts. There are no noticeable differences between the fresh catalyst and the reused one. It indicates the high recyclability of the catalyst.

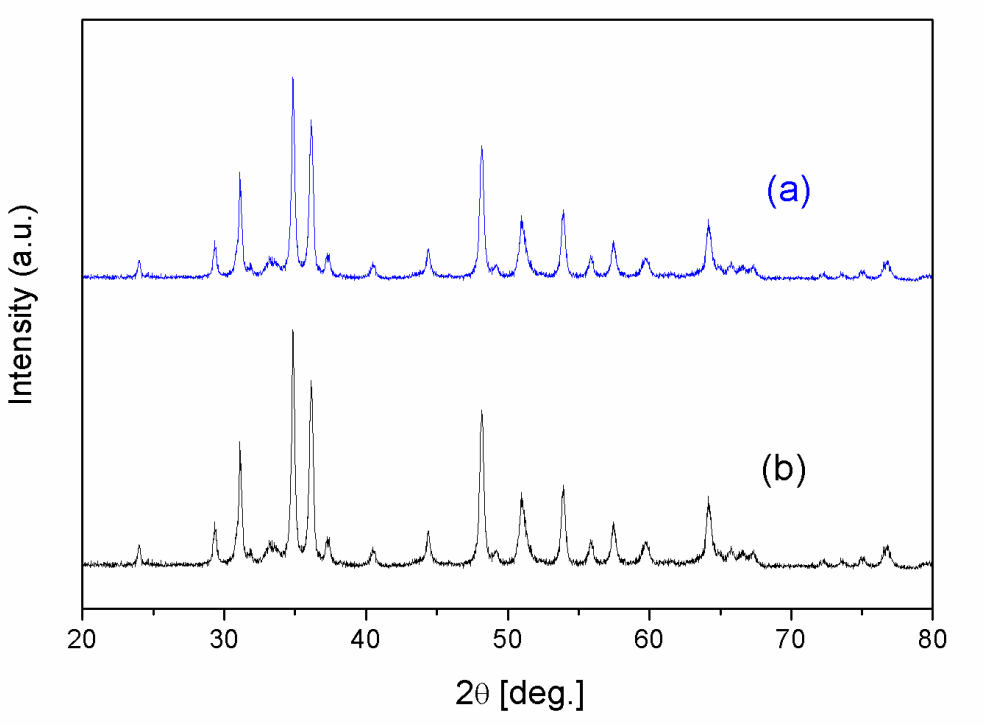

Figure S. 22 X-ray diffraction spectra of (a) fresh catalyst $FeSe_2$, (b) recovered $FeSe_2$ after 5th recycling in the reductive carbonylation reaction of NB.

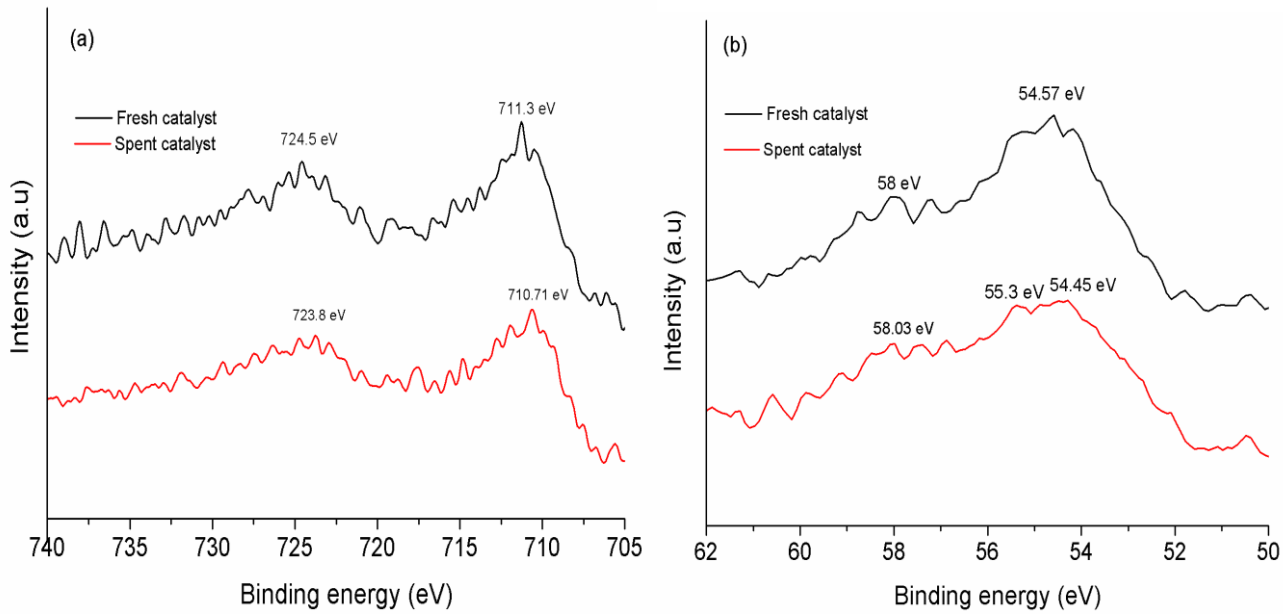

Figure S. 23 XPS of the fresh and spent $FeSe_2$/ γ-Al_2O_3 in the region of (a) Fe 3p; (b) Se 3d.

XPS results of fresh and spent $FeSe_2$/ γ-Al_2O_3 over the spectra regions of Fe 3p and Se 3d were showed in Fig. S21. In the Fe 3p region of fresh and spent catalysts, there was no difference in the binding energy. In the Se 3d region, the spent catalyst shows the shifting of Se 3d peak from 54.45 eV to 55.3 eV, it is indicating the partial formation of Se (0) species during the reductive carbonylation process. These results are in good agreement with the presence of carbonyl selenide (Se-CO) species, which was shown in FT-IR result.

References:

[1] Q. Zheng, X. Cheng, H. Li, Microwave Synthesis of High Activity FeSe2/C Catalyst toward Oxygen Reduction Reaction, Catalysts. 5 (2015) 1079-1091. https://doi.org/10.3390/catal5031079

[2] M. Shenasa, S. Sainkar, D. Lichtman, XPS study of some selected selenium compounds, J electron spectrosc. 40 (1986) 329-337. https://doi.org/10.1016/0368-2048(86)80043-3

[3] J. Jia, Q. Zhang, Z. Li, X. Hu, E. Liu, J. Fan, Lateral heterojunctions within ultrathin FeS–FeSe2 nanosheet semiconductors for photocatalytic hydrogen evolution, Journal of Materials Chemistry A. 7 (2019) 3828-3841. https://doi.org/10.1039/c8ta11456k